

# Studies of Corrosion using Scanning Kelvin Probe Force Microscopy and AFM Scratching

G. S. Frankel and P. Leblanc

*Fontana Corrosion Center, The Ohio State University  
477 Watts Hall, 2041 College Rd., Columbus, OH, 43210, USA*

The development of techniques linked to the atomic force microscope (AFM) has enabled the evaluation of physical and chemical properties of sub-micron structures. Scanning Kelvin Probe Microscopy (SKPFM) and in-situ AFM scratching have been particularly useful for studying corrosion phenomena. SKPFM generates a map of the potential distribution across a sample with a resolution of 100 nm. Furthermore, the open circuit potential of various pure metals in solution is linearly related to the Volta potential value measured in air immediately after exposure. SKPFM is a useful tool to assess the practical nobility of a surface. This technique has been successfully applied to the heterogeneous microstructure of AA2024-T3 and provided clear evidence regarding the shape, position, compositional inhomogeneities and local practical nobility of copper-rich intermetallic particles. The reactivity of these particles has been studied in detail. AFM scratching is an extremely controlled method to locally disturb the protective oxide film on a metal surface in solution. As with other approaches that utilize in situ scratching, the stability of the passive film and the tendency for stabilization of localized corrosion can be monitored. However, the lateral imaging capabilities of the AFM provides an approach to study the role of different microstructural features in the process of localized corrosion stabilization. Finally, AFM scratching can be used to open up small windows in a protective organic coating to reveal selected microstructural features. This allows the study of the corrosion behavior of these features in isolation from the rest of the microstructure or to study the interaction of different selected microstructural features. This approach is useful for understanding the interaction between different types of intermetallic particles in AA2024-T3.

**Keywords** : AFM, Al alloys, pitting corrosion, Kelvin probe

## 1. Introduction

Localized corrosion is usually driven by microstructural heterogeneities.<sup>1)</sup> For instance, in Al alloys, alloying elements added for increased strength are often segregated to and enriched in intermetallic particles. Such particles can be large constituent phases on the order of tens of microns in size, or precipitated hardening particles nm in size. Localized corrosion typically initiates at the larger particles (micron size or larger), but the role of the particle in the localized corrosion process depends on the particle type. In AA2024-T3, there exist two primary types of large intermetallic particles: AlCuFeMn particles and S phase Al<sub>2</sub>CuMg particles.<sup>2)</sup> The FeMn-containing particles have a range of composition and are often themselves heterogeneous. These particles are typically considered to be cathodic to the matrix.<sup>3)</sup> The S phase particles are more homogeneous, and are thought to be active owing to the high Mg concentration. It has been suggested that Mg and Al can dealloy from S phase particles, leaving a porous

Cu-rich residue that might break apart and redistribute Cu across the sample surface, providing a large active cathode.<sup>1)</sup>

Clearly, it is of interest to be able to understand the exact role of these intermetallic particles in the localized corrosion process. Owing to their small size, techniques with high spatial resolution are required to do so. A number of techniques with sub-micron resolution exist, such as SEM, EDS, AES, and TEM. This paper will summarize recent work utilizing a relatively new technique, the Scanning Kelvin Probe Force Microscope (SKPFM) to study the corrosion behavior of Al alloys.<sup>4-8)</sup> The SKPFM is an AFM-based technique with sub-micron resolution. It is a robust technique that is relatively quick and simple to perform. It simultaneously provides topographic and potential maps of the same region of a sample surface.

It has been shown that, for distances greater than 100 nm from the surface, the potential measured by SKPFM is constant,<sup>4)</sup> which corresponds to the conceptual defi-

nition of the Volta potential difference for a metal-solution interface. However, the separation between the influence of the surface dipoles and free charges contribution on the measured potential is theoretical and does not exist as such for a real solid-liquid interface. The influence of adsorbed dipoles dominates closer to the surface, but also influences the potential measured at distances equal to or greater than 100 nm. Nonetheless, the overall nature of the potential measured by SKPFM justifies the description of it as the Volta potential difference.

## 2. Experimental

Scanning Kelvin probe force microscopy was performed with commercial AFMs (Nanoscope IIIa or Dimension 3100, Digital Instruments). These instruments can measure the surface topography and potential distribution simultaneously on a line-by-line basis using metal-coated silicon cantilevers that are electrically conducting. The cantilevers were also obtained from Digital Instruments. The principle and details of the SKPFM measurement have been previously described. In short, it involves scanning the surface in tapping mode to determine the topography on a line-by-line basis. The cantilever is then lifted a fixed distance from the surface, typically 100 nm, and the tip is rescanned at this height in "lift mode". On the rescan, an AC voltage is applied to the tip, which stimulates oscillations of the cantilever in the presence of an electric field. The magnitude of the oscillations at the stimulating frequency, monitored by the AFM detection scheme, is nulled on a point-by-point basis on the rescan by adding a DC voltage that balances the field. This approach to potential distribution measurement is not possible in an aqueous solution because the large voltages applied to the tip would result in faradaic reactions. In this study, all potential mapping was performed in air. Since this technique is a nulling method, the output signal from the instrument was inverted; it has been shown previously that inversion of the signal is needed to obtain the expected polarity of the potential measurements. The values obtained are relative to the potential of the tip. The tips are only pseudo-references since their potential may vary with changes in the surface oxide. In order to avoid errors associated with variations in the tips or instabilities in the instrument electronics, the potential measurements were calibrated by comparison to the potential measured on a pure Ni surface after immersion in DI H<sub>2</sub>O. Ni was chosen as a reference because it was found to have a stable potential. All potential measurements are reported herein relative to that of a Ni sample. Consecutive measurements in air on a stable reference sample using different tips

coated with the same metal showed potential difference of less than 50 mV, giving an indication of the reproducibility of this method.

Samples were cut from an AA2024-T3 sheet (nominal composition 3.8-4.9% Cu, 1.2-1.8% Mg, 0.3-0.9% Mn, 0.5% Fe, 0.5% Si, 0.25% Zn, 0.1% Cr, 0.05% Ti, balance Al). A non aqueous lubricating slurry (Blue Lube by Struers) was used during the surface preparation (grinding and polishing). The AA2024-T3 disks were mechanically ground with successively finer SiC paper through 1200 grit and polished with 6, 3, and 1  $\mu$ m diamond paste. Prior to study, samples were cleaned ultrasonically with ethyl alcohol.

## 3. Results and discussion

### 3.1 Experiments on pure metals

In order to determine the usefulness of the scanning Kelvin probe force microscopy technique, potential measurements were made in air on a number of pure metal samples and compared to open circuit potential values determined on those samples immersed in aqueous solutions. The samples were immersed for 30 minutes in the solution before measurement to allow the open circuit potential to stabilize. Volta potentials are reported vs. the potential measured on a pure Ni sample, which served as a calibration standard. Ni was chosen as a reference because it was found to have a stable Volta potential. Fig. 1 shows the relationship of open circuit potential for different metals in deionized water, 0.5 M NaCl, and 0.1 M Na<sub>2</sub>SO<sub>4</sub> to the potential obtained in air with the Kelvin probe force microscope.<sup>4)</sup> For samples exposed to the chloride and sulfate solutions, both the open circuit potential in solution and the Volta potential difference in

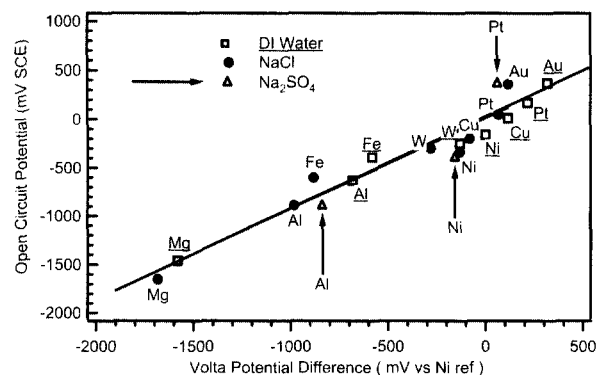
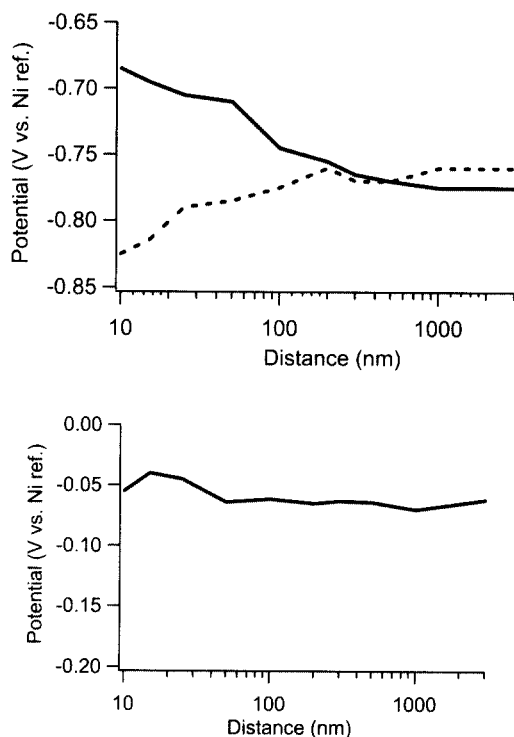


Fig. 1. Comparison of the potential measured in air by Scanning Kelvin Probe Force Microscopy with open circuit measured in solution: in DI water (squares and underlined elemental symbols), in 0.5 M NaCl solution (filled dots) and in 0.1 M Na<sub>2</sub>SO<sub>4</sub> (triangles and indicated with an arrow).<sup>4)</sup>

air after solution exposure were shifted in the active direction by around 150 mV relative to the values measured in and following DI water exposure. This suggests that adsorption of charged species at the electrode surface in chloride or in sulfate changed the dipole structure in the double layer and influenced the measured potential by the same value.

According to theoretical considerations, the measured potential should not be constant below 100 nm owing to the influence of image or dipole charges at the electrode surface.<sup>9)</sup> To investigate this, the influence on the measured potential of the dipoles in the interphase region was studied as a function of the vertical tip-sample distance. Fig. 2a shows the effect of tip-sample separation on the measured potential for pure Al directly after 30 min of immersion in DI water at OCP and one week later after storage in lab air.<sup>4)</sup> At separation distances greater than about 100 nm, the potential is similar for the two cases, and independent of distance. This distance dependence of the potential with a constant domain above 100 nm is in good agreement with the literature.<sup>9)</sup> It should be mentioned that this distance between the tip and the sample is not an absolute value because, during the tapping mode scan, the tip is already at a few tens of nm from the



**Fig. 2.** Potential measured as a function of tip-sample distance for a) pure Al after 30 min at OCP. Solid line, directly after removal from DI water, dashed line, 1 week later. b) pure Ni after 30 min of immersion in DI water at OCP.<sup>4)</sup>

surface. In any case, it seems that above 100 nm the measured potential is constant and can be assumed to be the Volta potential difference. However, close to the surface, the measured potential changes with tip-sample separation, and the trend is different at the two times. Adsorption phenomena might be responsible for this difference. Indeed, after one week of storage in air, the surface might dehydrate, which could change the dipole structure. The influence of the adsorbed layer on the potential/distance relationship varies considerably for different metals. Ni shows almost no distance dependence over the full range of separation distances, Fig. 2b.<sup>4)</sup> The potential on Ni is also independent of the time in air. This suggests the nickel oxide surface is very stable, and is the reason why Ni was chosen as a reference for the Volta potential difference measurements.

### 3.2 Spatial resolution

The advantage of the SKPFM over standard Scanning Kelvin Probes<sup>10),11)</sup> is the improved spatial resolution owing to the small size of the probe and the separation of the probe from the sample surface. Fig. 3 shows topographic and potential maps for a region of an as-polished sample of AA2024-T3.<sup>6)</sup> Considerable debris resulting from the non-aqueous polishing and rinsing of the sample, is visible in the topographic image on the left. Also visible are scratches and some holes that might have resulted from corrosion or particle pull-out. Finally, there are some raised regions associated with intermetallic particles that are harder than the alloy matrix and polish slower. On the right is the Volta potential map of the same region. The intermetallic particles are clearly evident with high contrast. Fig. 4 shows an SEM image of the same area.<sup>6)</sup> The bright spots in the SEM image were found by EDS analysis to be intermetallic particles. They match up perfectly with the high potential features in the potential map of Fig. 3. The large, blocky particles are the AlCuFe

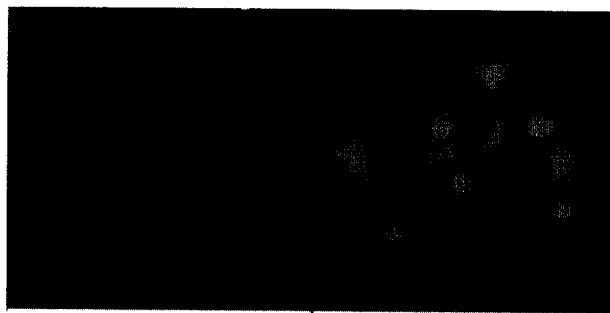


**Fig. 3.** AFM image of intermetallic particles in AA2024-T3. Both images 80 x 80  $\mu\text{m}$ , Left, topographical map with 100 nm z scale, right, Volta potential map with 1.5 V z scale.<sup>6)</sup>



Fig. 4. SEM image of the same region of the same sample as shown in Fig. 3.<sup>6)</sup>

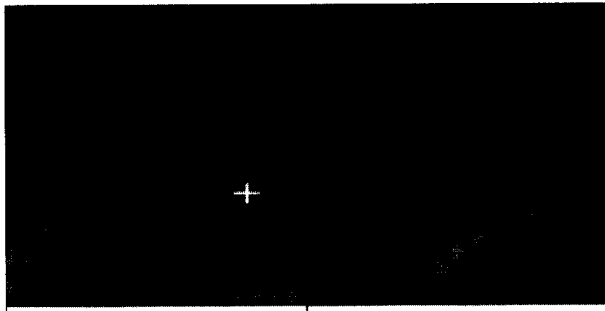


Fig. 5. Topographic (left, z scale 600 nm) and Volta potential (right, z scale 0.5 V) maps of a region of AA2024-T3 sample exposed to 0.5 M NaCl for 10 min. The area of both maps is  $1 \times 1 \mu\text{m}$ . An AlCuFeMn particle is located at the bottom right of the images.<sup>7)</sup>

Mn type and the three round particles, which are barely visible in the SEM image, are S phase particles. The secondary electron intensity in the SEM image is a convolution of topographic and chemical (z-number) effects. In contrast, the topographic and potential maps produced by the SKPFM separate these effects.

The limits of the spatial resolution capability of the SKPFM have not been fully investigated. Fig. 5 shows

an example of a small scan taken at the edge of an AlCuFeMn particle after exposure of the sample to 0.5 M NaCl for 10 min.<sup>7)</sup> Trenching of the matrix around the cathodic particle was observed as well as some attack within the particle. The region shown in Fig. 5 is the trench along the side of the particle, which is in the bottom left part of the Fig.. The trench is seen to be associated with a high potential, likely as a result of Cu enrichment. Potential and topographic features smaller than 100 nm can be seen in the images.

### 3.3 Behavior of particles in AA2024-T3

The high Volta potential exhibited by the S phase particles in the as-polished condition relative to the matrix (Fig. 3) is opposite of what would be expected given the relatively low potential reported for grains of S phase in a bulk fabricated analog sample<sup>3)</sup> and the correlation presented above relating Volta potential measured by the SKPFM to corrosion potential. Fig. 6 shows Auger depth profiles of the matrix, Al<sub>2</sub>CuMg and AlCuFeMn particles collected simultaneously on a sample of AA2024-T3 directly after polishing in a non-aqueous polishing slurry. The surface of the intermetallic particles was covered with Al-Mg oxide (or hydroxide); Cu was depleted on the surface of both kinds of particles relative to the concentration beneath the surface. This measurement indicates that the noble potentials observed on these types of particles after polishing using SKPFM are not caused by surface enrichment of copper as might be expected. A more complex behavior has to be considered.

The oxide film formed on the reactive S phase particles during non-aqueous polishing provides some protectiveness to the surface. It has been shown that S-phase particles do not dissolve immediately upon exposure to 0.1 or 0.5 M NaCl.<sup>5,7)</sup> The Volta potential of the different regions on the surface start out quite different, as evi

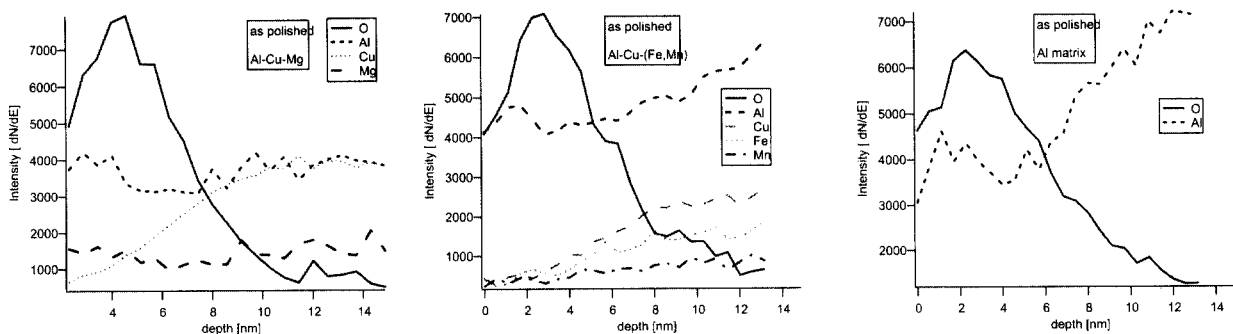


Fig. 6. AES depth profile of an AA2024-T3 sample after polishing in non aqueous solution: (a) S phase Al<sub>2</sub>CuMg particle, (b) AlCuFeMn particle and (c) Al matrix.

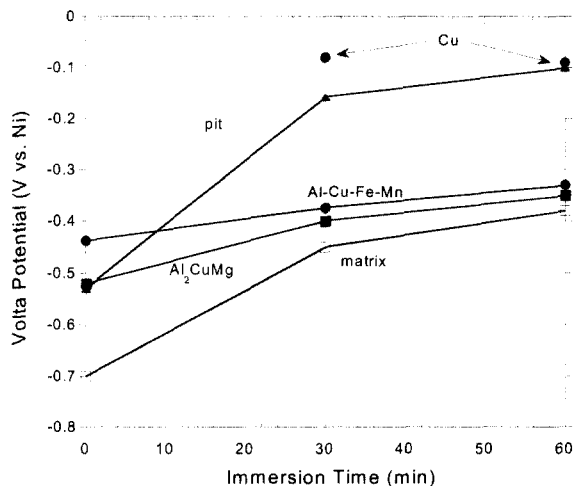


Fig. 7. Volta potential change of pits, uncorroded matrix and uncorroded intermetallic particles in AA2024-T3 following immersion in 0.5 M NaCl for different periods of time. Volta potential of Cu given for comparison.<sup>5)</sup>

denced by the contrast shown in potential map of the as polished sample. With time, these potentials merge to a single value and the contrast in the potential map decreases. This is shown in Fig. 7 for various regions of samples exposed to 0.5 M NaCl.<sup>5)</sup> Regions that are active pits go to a high potential similar in value to pure Cu exposed to the same solution. It was shown that S phase particles not associated with a pit in the as-polished condition are eventually attacked when their potential reaches a value similar to that of the matrix. At this point, the protectiveness of the oxide film on the particle is reduced and localized attack at the particle can commence.

Sputter etching of the as-polished surface can change the behavior of the S-phase particles.<sup>4),5)</sup> Partial removal of the oxide, as indicated by the O signal in the SAM tool in which the sputter etching was performed, resulted in the reversal in contrast for some, but not all, of the S-phase particles; after sputtering and exposure to air, they had a Volta potential lower than that of the matrix. Subsequent exposure to 0.5 M NaCl for 30 min resulted in dissolution of some, but not all, of the particles that had exhibited a low potential after sputter etching.<sup>5)</sup>

### 3.4 Small exposed areas

It is possible to expose small areas of a sample by coating the sample with a thin layer of a protective polymeric film and then scratching through the film at selected regions.<sup>5)</sup> In this fashion, it is possible to expose regions containing only certain microstructural features or ratios of such features that are different than that given by the alloy microstructure.

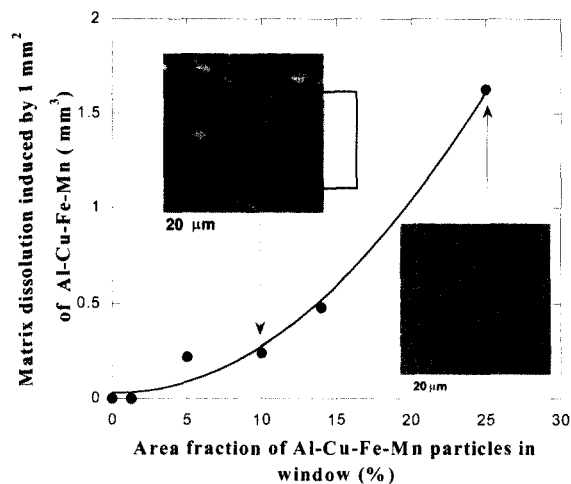


Fig. 8. Effect of area fraction of Al-Cu-Fe-Mn in exposed window on matrix dissolution after 60 min exposure to 0.5 M NaCl.<sup>5)</sup>

A window exposing an area containing only a portion of an AlCuFeMn particle exhibited no corrosion upon 2 h exposure to 0.5 M NaCl. When such a particle was exposed with some surrounding matrix (but no large S-phase particles), considerable attack was found, and the extent of the attack increased as the fraction of the exposed area taken up by the AlCuFeMn particle increased, Fig. 8.<sup>5)</sup> This is what might be expected by simple galvanic corrosion considerations. AlCuFeMn inclusions are efficient cathodic regions and can drive corrosion reactions, not only at active S-phase particles but also in the matrix.

Interestingly, when an area containing typical S phase particles and matrix (no AlCuFeMn particles) was exposed to 0.5 M NaCl, no attack was seen after 120 min. This is the same as was observed when only AlCuFeMn region was exposed. Clearly, localized corrosion only initiates in this system if there is simultaneous exposure of both active cathodes (AlCuFeMn particles) and an anodic site (S-phase particle or matrix). The absence of either anode or cathode prevents local attack. It should be noted that some S-phase particles were attacked when exposed to solution in a window that did not contain an AlCuFeMn particle. These reactive S phase particles were typically larger than average, and exhibited a lower Volta potential in the as-polished condition.

### 3.5 AFM Scratching

In situ scratching of a passive metal with a sharp stylus has been used to assess repassivation behavior by localized removal of the passive film.<sup>12-14)</sup> These and other studies have provided considerable insight into the nature of passivity and the kinetics of repassivation. Most of the prior work measured current transients generated under

potential control. The effect of any local heterogeneities cannot be studied by simple scratching as there is no control over the placement of the scratch relative to the microstructure. Pressure applied by an AFM tip on the surface of a sample during in situ contact mode rastering is a form of scratching on the micro scale. An AFM tip can be placed directly on a feature of interest as determined by the topography or by ex situ SKPFM and the use of fiducial marks. Furthermore, the force applied by a tip can be controlled exactly.

In situ AFM scratching has been used to probe a number of different aspects of the protectiveness of the oxide film formed on Al and on different particles in the microstructure of Al alloys.<sup>5,7,8,15</sup> A wide range of behavior was observed depending on the sample and the environment. Scratching of 99.99% Al or Al 1100 with a Si tip in the Nanoscope III environmental cell resulted in the formation of a smooth bottomed trench, Fig. 9.<sup>7,8</sup> The depth of the trench depended on the AFM photodiode setpoint voltage, which is a measure of the scratching force. It is interesting that scratching of pure Al in 0.5 M concentrated NaCl resulted in uniform dissolution at a high rate and not in the formation of pits, even though Al might not be expected to repassivate spontaneously in this solution.

An explanation for this behavior can be given based on the concept that a critical current density is necessary to sustain pitting and prevent repassivation.<sup>16</sup> The rate of dissolution in a pit is on the order of  $A/cm^2$  over the first fractions of a second following breakdown. At open circuit, the high dissolution rate must be accompanied by an equally high rate of cathodic reaction, which in aerated 0.5 M NaCl is primarily oxygen reduction. Since the volume of electrolyte in the AFM cell was rather small (about 0.1 ml) and the cell was sealed, the supply of

oxygen was finite and it quickly dropped to a level insufficient to maintain the required rate of anodic reaction. The result of continual film breakdown, accelerated dissolution and repassivation was the formation of a uniform trough. This is essentially erosion corrosion. This interpretation is supported by an experiment in which the 0.5 M NaCl solution was continually pumped through the AFM cell during scratching. Instead of accelerated uniform corrosion resulting in the formation of a flat-bottomed trough, scratching with solution flow at open circuit tended to result in sustained pitting.<sup>8</sup>

AFM scratching of AA2024-T3 in a more dilute chloride solution, 0.01 M NaCl, resulted in immediate dissolution of the S-phase particles,<sup>7</sup> even in a stagnant cell without pumping of the solution. The AlCuMnFe particles are apparently sufficiently catalytic to support enough cathodic reaction to sustain the localized attack even with a limited supply of oxygen.

#### 4. Conclusions

Scanning Kelvin Probe Force Microscopy and in situ AFM scratching were shown to be useful techniques for the study of localized corrosion.

- SKPFM provides a potential map, which can be considered to be a map of the Volta potential difference, and represents the practical nobility of the surface. The Volta potential measured by SKPFM on pure samples in air following immersion in solution varies approximately linearly with the corrosion potential measured in that solution. It is sensitive to the excess charge and adsorbed dipoles.

- SKPFM provides clear visualization of the intermetallic particles in high strength Al alloys. The potential on the various particles and matrix changes with exposure and is related to the corrosion processes.

- The use of small exposure areas created by scratching through a thin protective polymeric film allowed the investigation of individual components of the microstructure in AA2024-T3. Both an active anode and cathode are required for localized corrosion, and the extent of attack depended on the area ratios of the anodes and cathodes.

- In situ AFM scratching provides information on the stability of the passive film and the ability of the system to stabilize localized attack.

#### Acknowledgements

This work was supported by the United States Air Force Office of Scientific Research under contract No F49620-6-1-0479. The authors gratefully acknowledge the con-

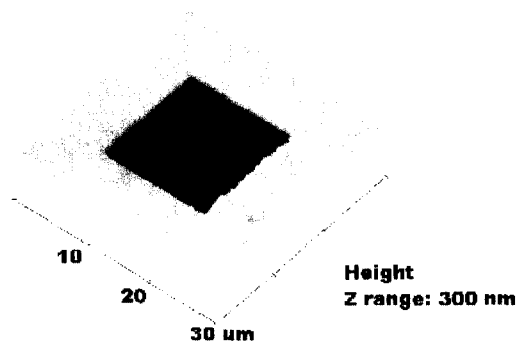


Fig. 9. In situ topographic map of a  $15 \mu\text{m}$  square hole in Al 99.99% obtained by contact mode scratching of the AFM tip in 0.5 M NaCl. Trench depth 75 nm.

tributions of Dr. Patrick Schmutz, who was intimately involved with much of the work during his tenure at OSU.

### References

1. R. G. Buchheit, R. P. Grant, P. F. Hlava, B. McKenzie, and G. L. Zender, *J. Electrochem. Soc.*, **144**, 2621 (1997).
2. V. Guillaumin and G. Mankowski, *Corr. Sci.*, **41**, 421 (1999).
3. R. G. Buchheit, *J. Electrochem. Soc.*, **142**, 3994 (1995).
4. V. Guillaumin, P. Schmutz, and G. S. Frankel, *J. Electrochem. Soc.*, **148**, B163 (2001).
5. P. Leblanc and G. S. Frankel, *J. Electrochem. Soc.*, submitted.
6. P. Schmutz and G. S. Frankel, *J. Electrochem. Soc.*, **145**, 2285 (1998).
7. P. Schmutz and G. S. Frankel, *J. Electrochem. Soc.*, **145**, 2298 (1998).
8. P. Schmutz and G. S. Frankel, *J. Electrochem. Soc.*, **146**, 4461 (1999).
9. J. O. M. Bockris and A. K. N. Reddy, Plenum Press, New York, (1970).
10. S. Yee, M. Stratmann, and R. A. Oriani, *J. Electrochem. Soc.*, **138**, 55 (1991).
11. M. Stratmann and H. Streckel, *Corros. Sci.*, **30**, 681 (1990).
12. G. T. Burstein and D. H. Davies, *Corr. Sci.*, **20** (1980).
13. G. T. Burstein and R. C. Newman, *Electrochim. Acta*, **25**, 1009 (1980).
14. G. T. Burstein and P. I. Marshall, *Corr. Sci.*, **23**, 125 (1983).
15. D. Devecchio, P. Schmutz, and G. S. Frankel, *Electrochem. Solid-State Lett.*, **3**, 90 (2000).
16. G. S. Frankel, J. R. Scully, and C. V. Jahnes, *J. Electrochem. Soc.*, **143**, 1834 (1996).